OPEN

PRS GLOBAL OPEN

ORIGINAL ARTICLE
Hand/Peripheral Nerve

Embryonic Stem Cell-Like Population in Dupuytren's Disease Expresses Components of the Renin-Angiotensin System

Nicholas On*
Sabrina P. Koh*
Helen D. Brasch, BMedSc, MBChB, FRCPA*
Jonathan C. Dunne, PhD*
James R. Armstrong, MBBS, MD, FRCS (Plast)*†
Swee T. Tan, MBBS, FRACS, PhD*†
Tinte Itinteang, MBBS, PhD*

Background: The renin-angiotensin system (RAS) mediates cardiac and renal fibrosis. Dupuytren's disease (DD) is a proliferative fibromatosis affecting the hands. This study investigated the expression of the RAS in DD.
Methods: 3,3-Diaminobenzidine (DAB) and immunofluorescent immunohistochemical (IHC) staining for (pro)renin receptor (PRR), angiotensin-converting enzyme (ACE), angiotensin II receptor 1 (ATIIR1), and angiotensin II receptor 2 (ATIIR2) was performed on 4-μm thick formalin-fixed paraffin-embedded sections of DD cords and nodules from 6 patients. Western blotting (WB) and NanoString mRNA analysis were performed to confirm RAS protein expression and transcriptional activation, respectively.
Results: IHC staining demonstrated the expression of PRR, ACE, ATIIR1, and ATIIR2 on the ERG$^+$ and CD34$^+$ endothelium of the micro vessels surrounding the DD cords and nodules. PRR was also expressed on the pericyte layer of these microvessels. WB confirmed protein expression of PRR, ACE, and ATIIR2 but not ATIIR1. NanoString analysis confirmed transcriptional activation of PRR, ACE, ATIIR1, but ATIIR2 was below detectable levels.
Conclusions: We demonstrated expression of PRR, ATIIR1, ATIIR2, and ACE on the embryonic stem cell–like cell population on the microvessels surrounding DD nodules and cords by IHC staining, although the expression of ATIIR1 was not confirmed by WB and that of ATIIR2 was below detectable levels on NanoString analysis. These findings suggest the embryonic stem cell–like cell population as a potential therapeutic target for DD, by using RAS modulators.
(Plast Reconstr Surg Glob Open 2017;5:e1422; doi: 10.1097/GOX.0000000000001422; Published online 24 July 2017.)

INTRODUCTION

Dupuytren's disease (DD) is a proliferative fibromatosis affecting the hands, causing shortening of the palmar fascia leading to contracture of the digits.[1] Patients may experience similar contracture in other areas, such as the plantar fascia (Ledderhose's disease) and penis (Peyronie's disease) in males.[1] The prevalence of DD varies worldwide, being most common in those of Northern European descent, with up to 30% reported in Norwegian men over 60 years.[2,3]

Current treatments for DD are unsatisfactory with high recurrence and complication rates.[4] Surgery is the mainstay treatment with fasciectomy being the most common procedure. Fasciectomy is associated with a recurrence rate of up to 39% over 5 years.[5] Dermofasciectomy reduces the recurrence rate to 12%.[6] Needle aponeurotomy has been used and recurrence rates of 50–58% have been reported.[5] Steroid injections have been used as a primary treatment or as an adjunct to surgery.[4,7] Injection of *Clostridium histolyticum* collagenase has been used recently

*From the *Gillies McIndoe Research Institute; and †Wellington Regional Plastic, Reconstructive, Maxillofacial and Burns Unit, Hutt Hospital, Wellington, New Zealand.*
Drs. Tan and Itinteang contributed equally to this work.
Received for publication August 12, 2016; accepted June 2, 2017.

DOI: 10.1097/GOX.0000000000001422

Disclosure: *Drs. Tan and Itinteang are inventors of a provisional patent application (no. 62/260,953) Treatment of Fibrotic Conditions. The authors are otherwise not aware of any commercial associations or financial relationships that might pose or create a conflict of interest with information presented in any submitted article. The Article Processing Charge was paid for by the Gillies McIndoe Research Institute general fund.*

Supplemental digital content is available for this article. Clickable URL citations appear in the text.

with a 10–31% recurrence rate[5] and significant complications including dermal atrophy, skin depigmentation, skin tears, and tendon rupture.[4,5,8]

Factors attributed to the development of DD include genetic predisposition, smoking, alcohol consumption, diabetes, liver cirrhosis, history of manual labor, and hand injury.[2] A possible autosomal dominant inheritance pattern has also been suggested.[2]

DD is characterized by the growth of highly cellular nodules, followed by avascular collagen rich cords.[9] Myofibroblasts are the predominant cell type within the DD nodules[9] and have been implicated in the development of DD.[9,10] They are involved in the production of α-smooth muscle actin and extracellular matrix reorganization, evident within DD tissues.[10]

A number of recent studies have shown an increased population of progenitor cells within DD tissues. Mesenchymal stem cells (MSCs), which possess the ability to differentiate into myofibroblasts,[11] have been observed in the overlying skin and surrounding fat of DD tissues.[12,13] We have recently demonstrated the presence of an embryonic stem cell (ESC)–like cell population, localized to the endothelium of the microvessels adjacent to DD nodules and cords.[14] This observation suggests the possibility of dysregulation of this stem cell population that ultimately sustains the proliferation of the myofibroblasts. The observation that dermofasciectomy, in which the overlying skin and surrounding tissue is also excised is associated with significantly lower recurrence rates compared with fasciectomy,[6] implicates the involvement of the overlying skin and surrounding adipose tissue in the disease process.

The renin-angiotensin system (RAS) is an endocrine[15] and paracrine system[16] that maintains cardiovascular homeostasis. It also plays a role in the mediation of fibrosis and healing of the skin, the kidneys, and the heart.[17–19] The RAS cascade begins with a renin-mediated cleavage of angiotensinogen (AGN) to the biologically inert angiotensin I. Angiotensin I is then cleaved by angiotensin-converting enzyme (ACE) to form angiotensin II (ATII),[15] which is the vasoactive end product of the RAS cascade and is a ligand for both angiotensin II receptor 1 (ATIIR1) and angiotensin II receptor 2 (ATIIR2).[15] (Pro)renin receptor (PRR, also known as ATP6AP2), a receptor for renin[20] binds both renin and its precursor (pro)renin.[20] Binding of renin to the PRR increases the efficiency of AGN cleavage.[20] PRR is also involved in multiple ATII-independent signaling pathways through its ligands, renin, and (pro)renin.[21]

We hypothesized that the RAS might be expressed by the ESC-like cell population in DD. In this study, we investigated the expression and localization of components of the RAS: PRR, ACE, ATIIR1, and ATIIR2 in DD tissues, using immunohistochemical (IHC) staining, Western blotting (WB), and NanoString mRNA analysis.

METHODS

Tissue Samples

Surgically excised DD samples from 6 male patients, aged 66–78 years (mean, 69.3 years) were sourced from the Gillies McIndoe Research Institute Tissue Bank, in a study approved by the Central Regional Health and Disability Ethics Committee (ref. no. 13NTB155). The DD tissue samples were separated into cords and nodules by the operating surgeon (J.R.A.).

Histochemical and IHC Staining

Hematoxylin and eosin staining was performed on 4-μm thick formalin-fixed paraffin-embedded sections of DD tissues from 6 patients to confirm the presence of DD cords and nodules, as recently reported.[14] 3,3-Diaminobenzidine (DAB) and immunofluorescent (IF) IHC staining was performed on sections of all DD cords and nodules using the Leica Bond Rx auto-stainer (Leica, Nussloch, Germany) with primary antibodies: PRR (1:2000; cat# AB40790, Abcam, Cambridge, Mass.), ACE (1:100; cat# 3C5, AbD Serotec, Oxford, United Kingdom), ATIIR1 (1:30; cat# AB9391, Abcam), and ATIIR2 (1:2000; cat# NBP1-77368, Novus Biologicals, Littleton, Colo.). Antibodies were diluted in Bond primary antibody diluent (Leica).

IF IHC staining was performed using a combination of VectaFluor Excel anti-rabbit 594 (ready-to-use; cat# VEDK-1594, Vector Laboratories, Burlingame, Calif.) and Alexa Fluor anti-mouse 488 (1:500; cat# A21202, Thermo Fisher Scientific, Waltham, Mass.) to detect combinations that included PRR and ATIIR2 and VectaFluor Excel anti-mouse (ready-to-use; cat# VEDK2488, Vector Laboratories) with Alexa Fluor anti-rabbit 594 (1:500; cat# A21207, Thermo Fisher Scientific) to detect combinations that included ACE and ATIIR1.

Human positive control tissues were placenta for PRR,[20] kidney for ACE,[22] and ATIIR1,[23] and liver for ATIIR2.[24] A DD nodule and a DD cord sample was used as a secondary antibody control by omitting the primary antibody.

Image Analysis

DAB IHC-stained slides were viewed and imaged with an Olympus DP21 digital camera (Olympus, Tokyo, Japan) fitted to an Olympus BX53 light microscope (Olympus). IF IHC-stained slides were viewed and imaged using an Olympus FV1200 confocal microscope (Olympus) and processed with CellSens Dimension 1.11 using 2D deconvolution algorithm (Olympus).

Western Blotting

Total protein was extracted from snap-frozen DD cord (n = 3) and DD nodule (n = 3) samples from 3 patients from the same cohort included for DAB IHC staining, by rotor-stator homogenization (Omni TH, Omni International, Kennesaw, Ga.) in ice-cold radioimmunoprecipitation assay buffer (Sigma-Aldrich, St. Louis, Mass.) supplemented with 1× HALT protease and phosphatase inhibitor cocktail (Pierce Biotechnology, Rockford, Ill.) and 10 mM dithiothreitol (Sigma-Aldrich). Soluble proteins were precipitated at -20°C for 1 hour (ProteoExtract Protein Precipitation Kit, Merck Millipore, Billerica, Mass.) and then resuspended at 4°C overnight in 1× sodium dodecyl sulfate sample buffer (Bio-Rad, Hercules, Calif.) containing 10 mM dithiothreitol. Protein samples (~30 μg total protein per sample) were resolved by 4–12% 1-dimensional polyacrylamide gel electrophoresis (Thermo Scientific, Waltham, Mass.) and

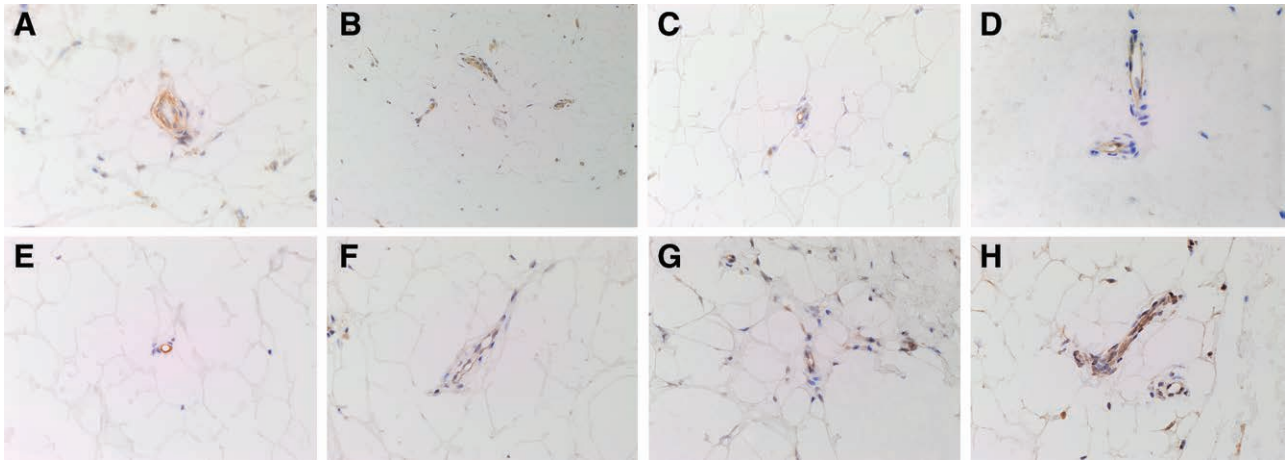

Fig. 1. DAB IHC-stained slides of representative DD cord (A, C, E, and G) and DD nodule (B, D, F, and H) samples showing the expression of PRR (A and B, brown), ACE (C and D, brown), ATIIR1 (E and F, brown), and ATIIR2 (G and H, brown) on the microvessels surrounding DD tissue. Expression of PRR, ACE, ATIIR1, and ATIIR2 was localized to the endothelium of these microvessels. PRR was also expressed on the surrounding pericyte layer (A and B). Nuclei were counter-stained with hematoxylin (A-H, blue). Original magnification: 400×.

transferred to PVDF membranes using an iBlot 2 (Thermo Scientific; n = 2). The membranes were blocked at 4°C for 90 minutes in tris-buffered saline (pH, 7.4) containing 0.1% Tween-20 (TBST) and 2% skim-milk powder and then probed at 4°C overnight using primary antibody diluted in TBST. Primary antibodies were ACE (1:200; cat# sc-12184, Santa Cruz, Rockford, Ill.), ATIIR2 (1:5000; cat# ab92445, Abcam), PRR (1:500; cat# HPA003156, Sigma-Aldrich), and β-actin (1:2000; cat# ab8226, Abcam). Membranes probed for ATIIR1, ATIIR2, PRR, and β-actin were then incubated at 4°C for 1 hour with the appropriate secondary antibody diluted in TBST, goat anti-rabbit, horseradish peroxidase (HRP) conjugate (1:20000; cat# A16110, Thermo Scientific), donkey anti-goat, HRP conjugate (1:5000; cat# ab97120, Abcam), or Alexa Fluor 647 rabbit anti-mouse (1:2000; cat# A21239, Thermo Scientific). Membranes probed for ACE were incubated at 4°C for 1 hour with rabbit anti-goat Superclonal biotin conjugate secondary antibody (1:20000, cat# A27013, Thermo Scientific) followed by incubation at 4°C for 20 minutes with streptavidin poly-HRP (1:5000, cat# 21140, Thermo Scientific). HRP detection was achieved using Clarity Western enhanced chemiluminescence substrate (Bio-Rad), and all membranes were imaged using a Chemi-Doc MP imaging system (Bio-Rad).

Nanostring mRNA Analysis

Snap-frozen DD cord (n = 5) and DD nodule (n = 5) samples from 5 patients from the same cohort included for DAB IHC staining were used to isolate total RNA. RNA was extracted using the MagJET RNA Kit and KingFisher Duo (ThermoFisher Scientific) protocol and quantitated by the NanoDrop 2000 Spectrophotometer (Thermo Scientific) and Qubit (Thermo Scientific). mRNA was assayed by New Zealand Genomics Ltd (Dunedin, NZ), using the NanoString nCounter Gene Expression Assay (NanoString Technologies, Seattle, Wash.). Probes for the genes were designed and synthesized by NanoString Technologies and are PRR (ATP6AP2, NM_005765.2), ACE (CD143, NM_000789.2), ATIIR1 (AGTR1, NM_000685.3), and ATIIR2 (AGTR2, NM_000686.3). Raw data were analyzed by nSolver software (NanoString Technologies) using standard settings and were normalized against the housekeeping gene glyceraldehyde 3-phosphate dehydrogenase (GAPDH).

RESULTS

Histochemical and 3,3-Diaminobenzidine IHC Staining

Hematoxylin and eosin staining confirmed the presence of DD cords and nodules on the slides and demonstrated the location of the microvessels. DAB IHC staining showed expression of PRR, localized to the endothelium and pericyte layer of the microvessels at the periphery of both the DD cords (Fig. 1A, brown) and nodules (Fig. 1B, brown). ACE was localized to the endothelium of these microvessels surrounding both the DD cords and nodules (Fig. 1 C, D, brown). Both the DD cords and nodules expressed ATIIR1 (Fig. 1 E, F, brown) and ATIIR2 (Fig. 1 G, H, brown).

Positive control staining was demonstrated in human placenta for PRR, kidney for ACE, liver for ATIIR1, and kidney for ATIIR2. There was minimal staining on the negative control (**see figure, Supplemental Digital Content 1**, which displays DAB IHC-stained positive control human samples using placenta for PRR (A, brown), kidney for ACE (B, brown), liver for ATIIR1 (C, brown), and kidney for ATIIR2 (D, brown). Negative control by omission of the primary antibody (E) confirmed specificity of the secondary antibody. Nuclei were counter-stained with hematoxylin (A-E, blue). Original magnification: 400x, ***http://links.lww.com/PRSGO/A483***).

IF IHC Staining

To confirm the localization of PRR, ATIIR1, ATIIR2, and ACE, we performed dual IF IHC staining on sections of DD nodule (n = 2) with the endothelial markers CD34 or ERG. PRR (Fig. 2A, red) was localized to the $CD34^+$ (Fig. 2A, green) endothelium of the microvessels and the pericyte

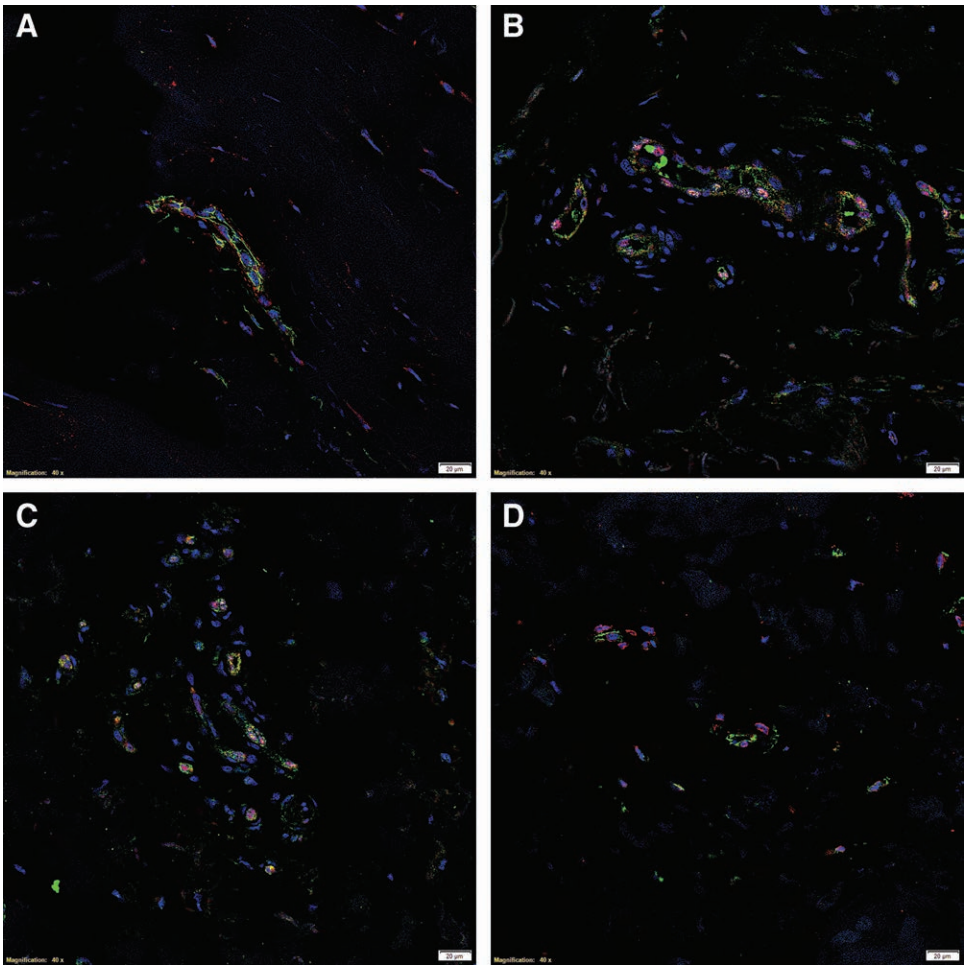

Fig. 2. IF IHC-stained slides of representative DD nodule samples showing coexpression of the endothelial marker CD34 (A, green) and PRR (A, red). PRR (A, red) was also expressed on the surrounding pericyte layer. Expression of ACE (B, green) and ATIIR1 (C, green) on the ERG+ endothelium (B and C, red) was also demonstrated. ATIIR2 (D, red) was also expressed on the endothelium expressing CD34 (D, green). Nuclei were counter-stained with 4′6-diamino-2-phenylindole (A–D, blue). Scale bars: 20 μm.

layer surrounding the endothelium. ACE (Fig. 2B, green) and ATIIR1 (Fig. 2C, green) were expressed on the ERG$^+$ (Fig. 2B, C, red) endothelium of the microvessels. ATIIR2 (Fig. 2D, red) was expressed on the nuclei of the CD34$^+$ (Fig. 2D, green) endothelial cells. (**see figure, Supplemental Digital Content 2**, which displays separated images of IF IHC-stained slides of representative DD nodule samples showing expression of PRR (A, red) on the endothelium of the microvessels that expressed CD34 (B, green) and the surrounding pericyte layer; the ERG$^+$ (C&E, red) endothelium expressed ACE (D, green) and ATIIR1 (F, green); and ATIIR2 (G, red) was expressed on the endothelium of the microvessels expressing CD34 (H, green). Nuclei were counter-stained with 4′6-diamino-2-phenylindole (A-H, blue). Scale bars: 20μm, ***http://links.lww.com/PRSGO/A484***).

WB

WB analysis of total protein extracts from snap-frozen DD cord (n = 3) and DD nodule (n = 3) samples from 3 patients confirmed the presence of PRR (Fig. 3A) at the expected size of 39 kDa in all samples. ACE (Fig. 3B) was detected by tertiary cascade WB at the expected ~190 kDa in 4 and 5 of the nodule and cord extracts, respectively. Similarly, ATIIR2 (Fig. 3C) was detected in most but not all 3 sets of DD total protein extracts, at ~50 kDa. ATIIR1 was not detected in any of the 3 set of DD samples examined (data not shown). β-Actin confirmed approximately equivalent loading of the 3 cord and 3 nodule DD samples (Fig. 3).

Nanostring mRNA Analysis

NanoString mRNA analysis for PRR, ACE, ATIIR1, and ATIIR2 in DD cords (n = 5) and DD nodules (n = 5) from 5 patients was performed, normalized against the housekeeping gene, GUSB. Transcriptional profiling confirmed the presence of PRR, ACE and ATIIR1 mRNA in all the samples but ATIIR2 mRNA was below detectable level within all the samples examined (Fig. 4).

DISCUSSION

In this study, we have demonstrated expression of PRR, ACE, ATIIR1, and ATIIR2, localized to the endothelium of

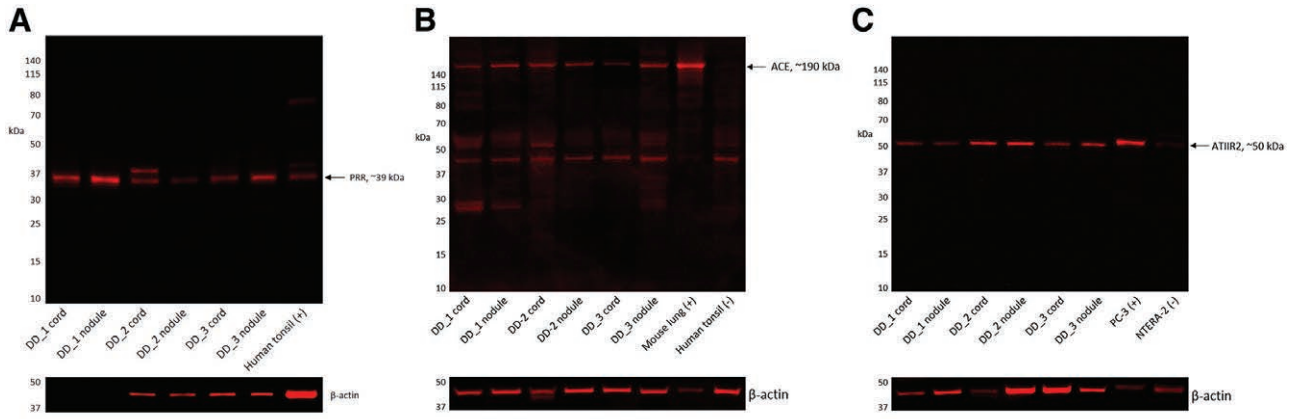

Fig. 3. Representative WB images of total protein extracted from 3 DD cord and 3 DD nodule tissues from 3 patients demonstrated the presence of PRR (A), ACE (B), and ATIIR2 (C). β-actin confirmed approximately equivalent protein load between samples (A–C).

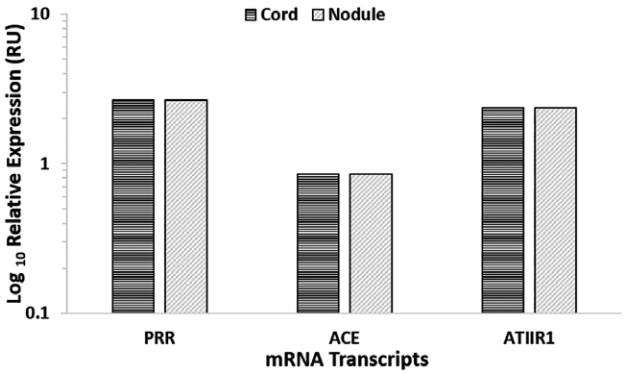

Fig. 4. Relative expression of RAS-related mRNA transcripts in DD cords (n = 5) and nodules (n = 5) depicted in RUs as a ratio over the GUSB housekeeper. ATIIR2 was below the detection level. RU, relative unit.

the microvessels in DD cords and nodules by IHC staining. PRR is also expressed by the pericyte layer. Although ATIIR1 and ATIIR2 were detected by both DAB IHC and IF IHC staining, ATIIR2 was below the detectable levels when analyzed by NanoString, possibly due to rapid clearance of the mRNA. Furthermore, ATIIR1 was not detected by WB.

Viil et al.[25] have demonstrated that DD-associated microvessels form proliferative centers that provide an abnormal microenvironment of cytokines and signaling factors. Iqbal et al.[12] have recently identified an MSC population with the ability to differentiate into myofibroblasts seen in DD nodules and cords, the skin overlying nodule and perinodular fat areas. We recently demonstrated the presence of a more primitive ESC-like cell population within the microvessels of the tissues surrounding the DD nodules and cords.[14] This progenitor cell population may sustain the ESC-like cell population with downstream MSCs that give rise to myofibroblasts in DD. RAS might play a role in the development of DD, given its involvement in other fibrotic conditions.[17,18] Our hypothesis that the RAS may be expressed by the ESC-like cell population is supported by the observation that low-dose enalapril leads to improvement in hypertrophic and keloid scars.[26]

There are few previous reports on the potential role of the RAS in DD tissues. These focused on the myofibroblasts and yielded contradictory results. McKirdy et al.[27] have demonstrated the presence of the ATIIR1 on the myofibroblasts, whereas Stephen[28] has found limited expression of ATIIR1 and a much wider distribution of ATIIR2. Rayan et al.[29] show contraction in cultured DD myofibroblasts treated with ATII.

Renin cleaves AGN into ATI, with a 5-fold increase in the rate of cleavage when renin is bound to the PRR.[20] ACE then converts ATI into ATII, which acts on the ATIIR1 and ATIIR2 to regulate multiple signaling pathways.[15] We speculate that RAS signaling at the microvessels may contribute to the proliferative niche, which may promote the development of an ESC-like phenotype from which DD myofibroblasts may be ultimately derived.

PRR may also contribute to the dysregulation of signaling pathways independent of ATII. Binding of (pro)renin triggers intracellular signaling through the mitogen-activated protein kinases ERK1/2.[21] This can lead to the upregulation of profibrotic factors including transforming growth factor-β (TGF-β) and cyclooxygenase 2.[21] Furthermore, PRR associated with V-ATPase is involved in the canonical Wnt/β-catenin pathway.[30] The canonical Wnt pathway is linked to the TGF-β pathway, and together they are believed to play a key role in the pathogenesis of fibrotic diseases.[31] Wnt-signaling has been shown to be highly dysregulated in DD.[32]

We have demonstrated the presence and localization of components of the RAS in the ESC-like population on the microvessels within DD in the vicinity of the proliferating myofibroblasts. These results suggest that the ESC-like cell population, the proposed origin of the DD, may be a novel therapeutic target by modulating the RAS.

Swee T. Tan, ONZM, MBBS, PhD, FRACS
Gillies McIndoe Research Institute
PO Box 7184
Newtown 6424
Wellington
New Zealand
E-mail: swee.tan@gmri.org.nz

ACKNOWLEDGMENTS

We thank Ms. Liz Jones and Ms. Alice Chibnall of the Gillies McIndoe Research Institute for their assistance in immu-

nohistochemical staining and performing tissue processing for NanoString mRNA analysis, respectively. N.O. and S.K. were supported by summer scholarships from the Deane Endowment Trust. Ethical approval was obtained from the Central Regional Health and Disability Ethics Committee (ref. no. 13NTB155).

REFERENCES

1. Bayat A, McGrouther DA. Management of Dupuytren's disease—clear advice for an elusive condition. *Ann R Coll Surg Engl.* 2006;88:3–8.
2. Hindocha S, McGrouther DA, Bayat A. Epidemiological evaluation of Dupuytren's disease incidence and prevalence rates in relation to etiology. *Hand (N Y).* 2009;4:256–269.
3. Mikkelsen OA. The prevalence of Dupuytren's disease in Norway. A study in a representative population sample of the municipality of Haugesund. *Acta Chir Scand.* 1972;138:695–700.
4. Sweet S, Blackmore S. Surgical and therapy update on the management of Dupuytren's disease. *J Hand Ther.* 2014;27:77–83; quiz 84.
5. Chen NC, Srinivasan RC, Shauver MJ, et al. A systematic review of outcomes of fasciotomy, aponeurotomy, and collagenase treatments for Dupuytren's contracture. *Hand (N Y).* 2011;6:250–255.
6. Armstrong JR, Hurren JS, Logan AM. Dermofasciectomy in the management of Dupuytren's disease. *J Bone Joint Surg Br.* 2000;82:90–94.
7. Meek RM, McLellan S, Reilly J, et al. The effect of steroids on Dupuytren's disease: role of programmed cell death. *J Hand Surg Br.* 2002;27:270–273.
8. Rayan GM. Nonoperative treatment of Dupuytren's disease. *J Hand Surg Am.* 2008;33:1208–1210.
9. Rayan GM. Dupuytren disease: anatomy, pathology, presentation, and treatment. *J Bone Joint Surg Am.* 2007;89:189–198.
10. Musumeci M, Vadalà G, Russo F, et al. Dupuytren's disease therapy: targeting the vicious cycle of myofibroblasts? *Expert Opin Ther Targets.* 2015;19:1677–1687.
11. Quante M, Tu SP, Tomita H, et al. Bone marrow-derived myofibroblasts contribute to the mesenchymal stem cell niche and promote tumor growth. *Cancer Cell.* 2011;19:257–272.
12. Iqbal SA, Manning C, Syed F, et al. Identification of mesenchymal stem cells in perinodular fat and skin in Dupuytren's disease: a potential source of myofibroblasts with implications for pathogenesis and therapy. *Stem Cells Dev.* 2012;21:609–622.
13. Hindocha S, Iqbal SA, Farhatullah S, et al. Characterization of stem cells in Dupuytren's disease. *Br J Surg.* 2011;98:308–315.
14. Koh SP, On N, Brasch HD, et al. Embryonic stem cell-like population in Dupuytren's disease. *Plast Reconstr Surg Glob Open.* 2016;4:e1064.
15. Atlas SA. The renin-angiotensin aldosterone system: pathophysiological role and pharmacologic inhibition. *J Manag Care Pharm.* 2007;13:9–20.
16. Lavoie JL, Sigmund CD. Minireview: overview of the renin-angiotensin system—an endocrine and paracrine system. *Endocrinology.* 2003;144:2179–2183.
17. Mezzano SA, Ruiz-Ortega M, Egido J. Angiotensin II and renal fibrosis. *Hypertension.* 2001;38:635–638.
18. Rosenkranz S. TGF-beta1 and angiotensin networking in cardiac remodeling. *Cardiovasc Res.* 2004;63:423–432.
19. Sun Y, Ramires FJ, Zhou G, et al. Fibrous tissue and angiotensin II. *J Mol Cell Cardiol.* 1997;29:2001–2012.
20. Nguyen G, Delarue F, Burcklé C, et al. Pivotal role of the renin/prorenin receptor in angiotensin II production and cellular responses to renin. *J Clin Invest.* 2002;109:1417–1427.
21. Nguyen G, Muller DN. The biology of the (pro)renin receptor. *J Am Soc Nephrol.* 2010;21:18–23.
22. Uhlén M, Fagerberg L, Hallström BM, et al. Proteomics. Tissue-based map of the human proteome. *Science.* 2015;347:1260419.
23. Dinh DT, Frauman AG, Johnston CI, et al. Angiotensin receptors: distribution, signalling and function. *Clin Sci (Lond).* 2001;100:481–492.
24. Bataller R, Sancho-Bru P, Ginès P, et al. Activated human hepatic stellate cells express the renin-angiotensin system and synthesize angiotensin II. *Gastroenterology.* 2003;125:117–125.
25. Viil J, Maasalu K, Mäemets-Allas K, et al. Laminin-rich blood vessels display activated growth factor signaling and act as the proliferation centers in Dupuytren's contracture. *Arthritis Res Ther.* 2015;17:144.
26. Iannello S, Milazzo P, Bordonaro F, et al. Low-dose enalapril in the treatment of surgical cutaneous hypertrophic scar and keloid—two case reports and literature review. *MedGenMed.* 2006;8:60.
27. McKirdy SW, Chew BK, Tzaffetta K, Naylor IL, Sharpe DT. Angiotensin receptors in Dupuytren's tissue: Implications for the pharmacological treatment of Dupuytren's disease. *Br J Hand Ther.* 2001;6:79–83.
28. Stephen C. The effects of angiotensin-converting enzyme inhibitors as a pharmacological treatment for Dupuytren's disease. University of Central Lancashire: Preston (UK); 2013.
29. Rayan GM, Parizi M, Tomasek JJ. Pharmacologic regulation of Dupuytren's fibroblast contraction in vitro. *J Hand Surg Am.* 1996;21:1065–1070.
30. Krop M, Lu X, Danser AH, et al. The (pro)renin receptor. A decade of research: what have we learned? *Pflugers Arch.* 2013;465:87–97.
31. Akhmetshina A, Palumbo K, Dees C, et al. Activation of canonical Wnt signalling is required for TGF-β-mediated fibrosis. *Nat Commun.* 2012;3:735.
32. van Beuge MM, Ten Dam EJ, Werker PM, et al. Wnt pathway in Dupuytren disease: connecting profibrotic signals. *Transl Res.* 2015;166:762–771.e3.